Propagation Research in Japan

By Hiromitsu Wakana

Communications Research Laboratory, MPT
893-1 Hirai, Kashima, Ibaraki 314 Japan

Abstract L-band propagation measurements for land-mobile, maritime and aeronautical satellite communications have been carried out by using the Japanese Engineering Test Satellite-Five (ETS-V) which was launched in August 1987. This paper presents propagation characteristics in each mobile satellite communications channel.

1. Introduction

In the Communications Research Laboratory, propagation research has been carried out for many years by using various satellite beacons at many different frequencies. Since the launch of the ETS-V satellite, L-band propagation measurements are mainly being carried out for future mobile-satellite communications systems. This paper presents experimental results of propagation characteristics for vehicles, trains, airplanes and vessels.

Propagation effects between a geostationary satellite and mobile earth stations are: (1) blockage and shadowing (2) multipath scattering and reflections (3) ionospheric scintillation or Faraday rotation, and (4) Doppler frequency shifts.

In land-mobile satellite channel, multipath fading, shadowing and blockage from roadside trees, utility poles, buildings and terrains are typical problems. Maritime satellite channel has multipath fading caused by reflections from the sea surface at low elevation angles. In aeronautical satellite channel, multipath fading is caused by reflection from the sea surface and from airplanes' wings. It is shown that ionospheric scintillation is still of significance at frequencies above 1GHz and can impair mobile satellite communications channels.

2. Land-mobile satellite communications channel

2.1 Propagation characteristics for motor cars

L-band left-hand circularly polarized CW transmitted from the ETS-V satellite was received at a propagation measurement van with various antennas. Elevation angles of measurements along urban, suburban and rural roads and freeways are about 46 to 47 degrees.

Figure 1 shows a cumulative distribution of a receiving signal power with respect to the line-of-sight level, measured by a mechanically stirred four-element spiral array antenna (12dBi). Data were sampled with equidistance sampling pulses of a period of 3.14cm. Therefore, the results are independent of the vehicle speed.

Data in Tokyo urban areas show the fades of more than 5dB at the 33% probability level, which are mostly caused by blockage by ten-storied buildings and shadowing due to roadside

trees and utility poles. At a suburban area, it is found that for 13% of the distance the fade exceeds 5dB due to trees, utility poles and houses. On the other hand, the fade exceeds 5dB at only 3% probability along freeways. Main obstacles are overpasses and trees.

Figure 2 shows probability density functions of the received signal. It shows that the fade statistics can be divided into two parts. One is statistically described by a Rician distribution around the line-of-sight level. In mobile satellite channels, when both a dominant line-of-sight signal and scattered signal are received, the composite signal has a Rician distribution. The other is characterized by the fades larger than about 6 to 8dB, which are caused by blockage and shadowing. These data show that an effective fading margin is about 5dB for land-mobile satellite channels, although this value may depend on gains or patterns of the vehicle's antennas.

Based on a given threshold of a signal level, it can be determined whether a propagation channel is on a fade state (below the threshold) or on a non-fade state (above the threshold). Figures 3 and 4 show cumulative distributions of fade and non-fade durations, respectively. In Tokyo urban areas, the fade state continues over 10 meters at the 8% probability for all the fade-duration distributions. Such long fades are caused by blockage from buildings. Cumulative distributions of fade duration in suburban areas and freeways show moderate vegetative shadowing and can be presented by a lognormal fit (Vogel et al., 1989; Hase et al., 1991).

Except data in freeways, cumulative distributions of non-fade durations can be also approximated with the cumulative distribution of the lognormal distribution, which differs from that measured in Australia by Vogel et al. (1989).

Figure 5 shows a receiving noise measured in urban areas with omni-directional, mechanically stirred and phased array antennas. Impulsive noise, most of which may be generated by ignition of motorcars or motorcycles, has been observed, except for the phased array antenna. It shows that this effect depends on radiation patterns of mobile antennas. As a result of measuring bit error rates with 4.8kbps BPSK, it is found that this impulsive noise causes bit errors. In urban areas, impulsive noise is one of the effects which impair mobile communication channels.

2.2 Propagation characteristics for trains

A new satellite-based train control system is going to be introduced. In train-satellite communications channels, blockage and shadowing due to power poles, overpasses and noise generated from pantographs and motors impair communications quality. Figure 6 shows measured C/No (carrier-to-noise-power-density ratio) with an omni-directional antenna installed away from pantographs. Blockage due to trolley beams occurred periodically but impulsive noise was not observed. Except for blockage due to bridge's structures, overpasses and tunnels, durations of most fades are very short. The cumulative distribution shows the fades of more than 5dB at the 5% probability level.

3. Aeronautical satellite communications channel

In the CRL's experiment, the aircraft earth station was installed on a B-747F freighter of Japan Air Lines. A phased-array antenna of G/T of about 13dB/K was installed on the top of the fuselage. In-flight experiments were started in November 1987 and were conducted 24 times until March 1989, mainly on flight routes between Narita and Anchorage (Ohmori, 1990).

Most data show constant C/No and no fading except the period when the direction of the ETS-V satellite coincides with that of the main wings. Figure 7 shows standard deviations of signal levels versus antenna-beam directions and Figure 8 shows antenna-beam directions during flights between Narita and Anchorage and between Narita and Singapore. These figures show that signal level fluctuations occur only when antenna-beam directions coincide with that of the main wings and are caused by reflections from the main wings, vibrations of the wings and rolling of the airplane. Except at very low elevation angles below 0°, fading caused by reflections from the sea surface has never been detected. The reason is that waves reflected from the sea surface are blocked out by the fuselage and wings.

Yasunaga et al. (1989) have carried out propagation measurements using a helicopter with several antennas installed at both sides of the fuselage. Figure 9 shows statistics of multipath fading caused by sea reflections as a function of elevation angles. At an altitude of 10km and 5° elevation angle, the 99% fading level is less than that in the maritime satellite channel only by 2dB.

4. Maritime satellite communications channel

Multipath fading characteristics in maritime satellite communications channels have been studied by many authors and a lot of the literature has been published (Sandrin and Fang, 1986). Here, we present a brief introduction of our ETS-V's experiments. The ship earth station employs an improved short-backfire antenna of 40 cm in diameter (antenna gain of 15dBi) and has a two-axis mount (AZ/EL) with a program tracking function slaved to the ship-borne navigation system. It can compensate ship motions and keep the antenna pointing toward a satellite with a motion detector installed at the center of gravity of the ship. The CRL has developed a multipath fading reduction technique by using reflected cross-polarized components (Ohmori and Miura, 1983).

Figure 10 shows cumulative distributions of the received signal at several elevation angles. These data are found to be a good fit to the Rician distribution with a Rice factor, which is the direct-power-to-multipath-power ratio, of 5-9 dB, 6-12 dB and 15 dB at 3°, 6° and 10° elevation angles, respectively.

The generalized model for fading statistics proposed by Sandrin (1986) is described for antennas with gains ranging from 0 to 16 dBi as follows:

$$K = El + 4 \qquad \text{for } 2° < El < 4°,$$

where K is the Rice factor in decibels and El is an elevation angle in degrees. Therefore, as shown in Fig. 10, our measured data can be fit into this relationship at elevation angles less than 10 degrees.

Figure 11 shows a cumulative distribution of the C/No with respect to the medium of the C/No measured without the fading reduction technique. The fading depth is improved from 10.9 dB to 1.4 dB by the fading reduction technique. Both cumulative statistics without and with the fading reduction follow the Rician distribution with Rice factors of 6 dB and 20 dB, respectively. An increase of the Rice factor indicates reduction of reflected co-polarized components. This technique has a definite advantage at elevation angles lower than 6°.

5. Ionospheric scintillation

Figure 12 shows ionospheric scintillation measured on 30 November 1988 (Wakana and Ohmori, 1991). Both enhancement and negative fades with respect to the line-of-sight level were observed. The maximums of enhancement and fades are 6dB and -34dB, respectively. Mobile-satellite communication systems have only a small link-margin of about 4dB. Therefore, the fade due to ionospheric scintillation provides serious impairment in mobile-satellite communication channels.

Figure 13 shows observed places, frequencies and periods when the scintillation occurred. The data were measured by using signals transmitted from several satellites at different frequencies. Numbers above the periods show peak-to-peak variations of the signal level in decibels. As shown in this figure, ionospheric scintillation started simultaneously from low to middle latitudes at different frequencies, except at the Kashima earth station. The scintillation was observed even at the frequencies of 20GHz: this frequency is the highest frequency of ionospheric scintillation observed in Japan until now.

Since the ETS-V satellite is not always transmitting a beacon, we cannot monitor the propagation condition continuously. However, we have observed scintillation of about 2dB once every several months. From a satellite communication point of view, service availability which is the fraction of time that satisfactory satellite service is obtained on demand, is very important for users. Typically, systems in the fixed-satellite services are expected to achieve availability of 99.9% or better. Therefore, large attenuations produced by rare events of ionospheric scintillation can be ignored for the mobile satellite system design.

6. Conclusions

Mobile satellite communications experiments using the ETS-V satellite have provided fruitful experimental data about communication qualities and propagation characteristics. This paper presents the results of propagation measurements for land-mobile, aeronautical and maritime satellite communications.

In land-mobile satellite channels, blockage and shadowing by trees, buildings and terrains are a serious impairment rather than multipath fading , and a large link margin to combat blockage and shadowing is ineffective for providing acceptable services. Other aspects such as fade rate, fade and non-fade duration, delay spread and impulsive noise are important for the error correction scheme, data rate and data format.

In aeronautical satellite channels, propagation conditions are superior to those of land-mobile and maritime satellite channels because of no obstacles in link between a satellite and mobile stations. It was found that multipath fading due to sea-surface reflections can be ignored when the antenna is installed on the top of the fuselage, while a small amount of fading occurred due to reflections from main wings.

For maritime satellite channels, multipath fading statistics due to reflections from the sea surface are presented. Fading statistics can be modeled by the Rician model for most of the time. Furthermore, a technique to combat multipath fading which is applicable to commercial maritime communications links is presented.

Ionospheric effects are very important for radio communications systems operated at the frequencies below 1GHz. It was shown that this effect is still of significance at frequencies above

1GHz and can impair mobile satellite channel. However, from service availability point of view, large attenuation produced by rare events can be ignored for the mobile satellite system design.

References

Hase, Y., Vogel, W. J. and Goldhirsh, J., "Fade Duration derived from Land-Mobile-Satellite Measurements in Australia," IEEE Trans. Commun. (forthcoming).

Ohmori, S. and Miura, S., "A Fading Reduction Method for Maritime Satellite Communications," IEEE Trans. Antennas Propagat., vol. AP-31, No.1, pp. 184-187, Jan. 1983.

Ohmori, S., Hase, Y. and Wakana, H., "The World's First Experiments on Aeronautical Satellite Communications using the ETS-V Satellite," Denshi Tokyo, No. 29, pp.113-116, 1990.

Sandrin, W.A. and Fang, D.J., "Multipath Fading Characterization of L-band Maritime Mobile Satellite Links," Comsat Tech. Rev., Vol.16, No.2, pp.319-338, Fall 1986.

Yasunaga, M., Karasawa, Y., Matsudo, T. and Shiokawa, T., "Characteristics of Multipath Fading due to Sea Surface Reflection in Aeronautical Satellite Communications," Trans. IEICE, B-II, Vol. J72-B-II No. 7, pp.297-303, July 1989. (in Japanese)

Vogel, W. J., Goldhirsh, J. and Hase, Y., "Land-mobile-satellite propagation measurements in Australia using ETS-V and INMARSAT-Pacific," Johns Hopkins University, Applied Physics Laboratory Tech. Rep. S1R89U-037, August 1989.

Wakana, H., Ikegami, T., Kawamata, F., Ide, T. and Matsumoto, Y., "Experiments on Maritime Satellite Communications using the ETS-V Satellite," J. Commun. Res. Lab. (to be published).

Wakana, H. and Ohmori, S., "Signal Variation due to Ionospheric Scintillation on L-band Mobile Satellite Channels," Electronics Letters (submitted).

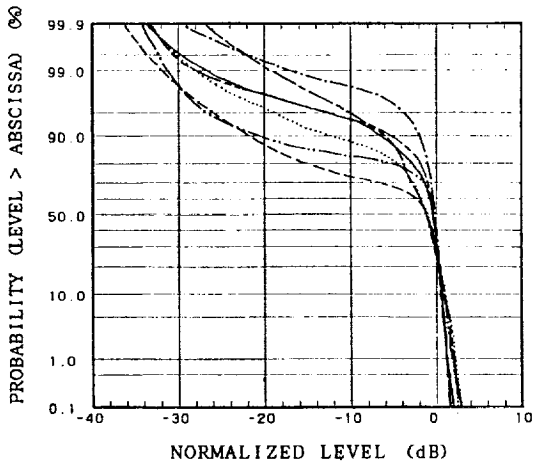

Figure 1 Cumulative distribution of receiving signal powers with respect to the line-of-sight level, measured by a mechanically stirred antenna of 12 dBi.

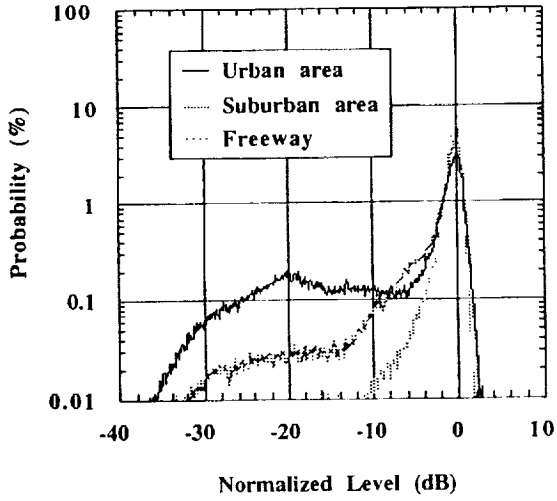

Figure 2 Probability density of receiving signal powers with respect to the line-of-sight level, measured by a mechanically stirred antenna of 12 dBi.

- Higashi-kantou (expressway, Ibaraki)
- Ohno village (rural area, Ibaraki)
- Tachikawa city (suburban area, Tokyo)
- Mito city (urban and suburban area, Ibaraki)
- Kyoto city (urban and suburban area, Kyoto)
- Chiba city (urban area, Chiba)
- Oumekaidou-Yasukunidohri (urban area, Tokyo)

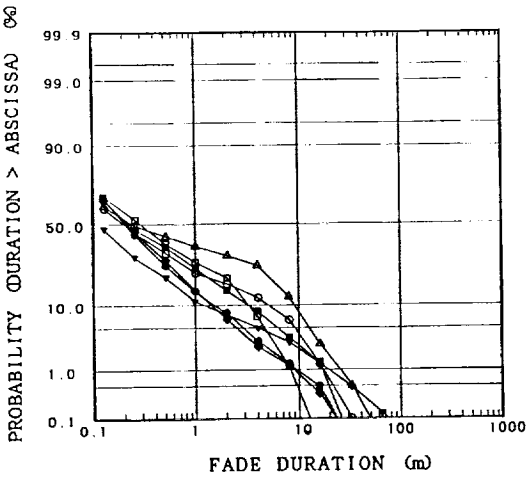

Figure 3 Cumulative distribution of fade duration: threshold level=-4dB.

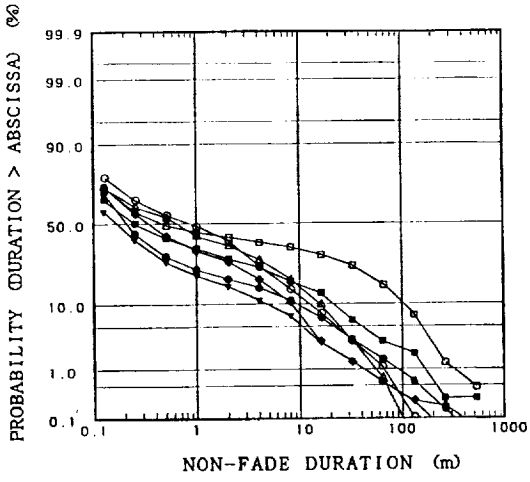

Figure 4 Cumulative distribution of non-fade duration: threshold level=-4dB.

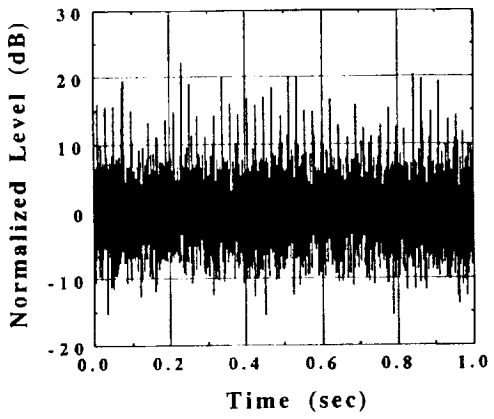

Figure 5 Receiving noise measured by an omni-directional antenna.

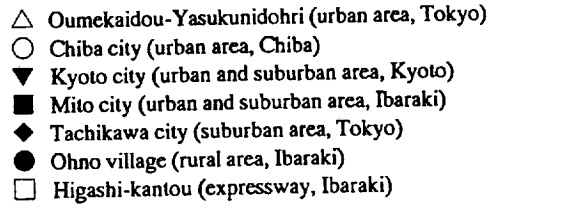

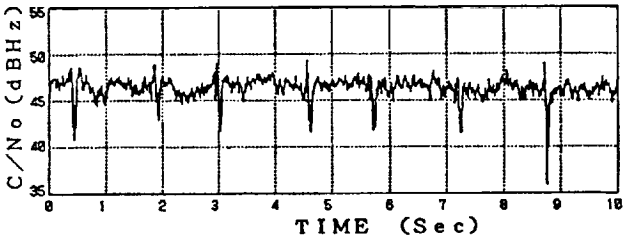

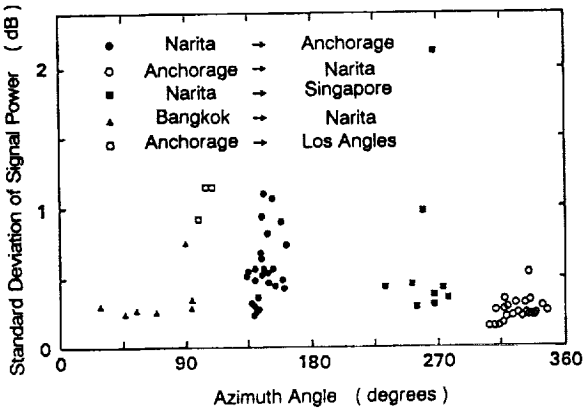

Figure 7 Standard deviation of signal level versus azimuth angle.

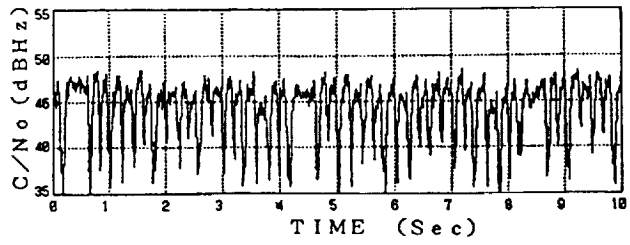

Figure 6 C/No measured on a train with an omni-directional antenna.

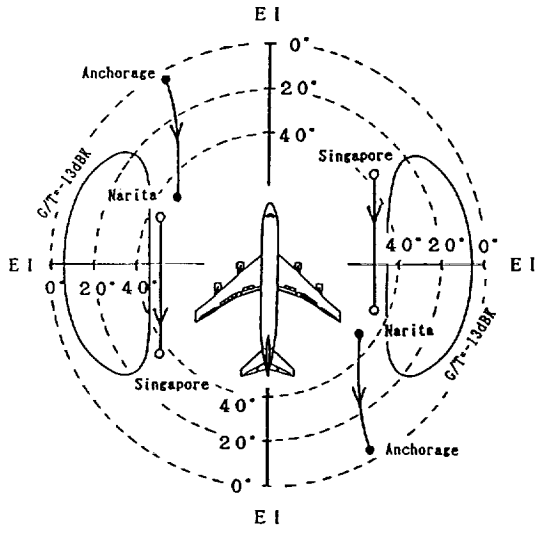

Figure 8 Antenna-beam direction during flight.

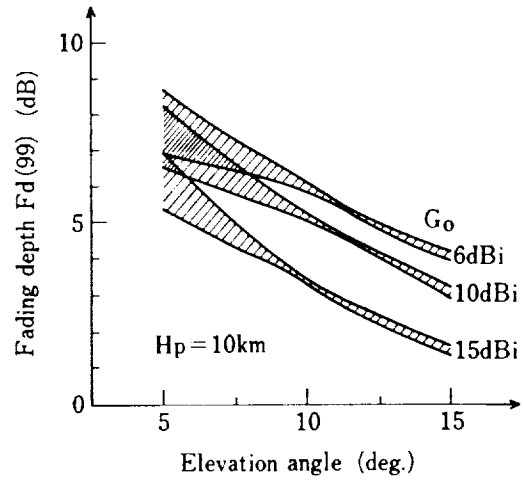

Figure 9 Fading depth versus elevation angle under rough sea condition

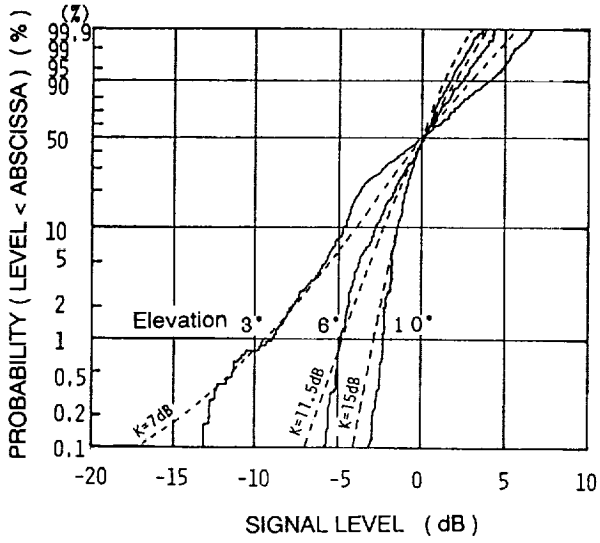

Figure 10 Cumulative distributions of receiving signal power with respect to the medium value. Dashed lines are the Rician distribution with several Rice factors (referred to as K).

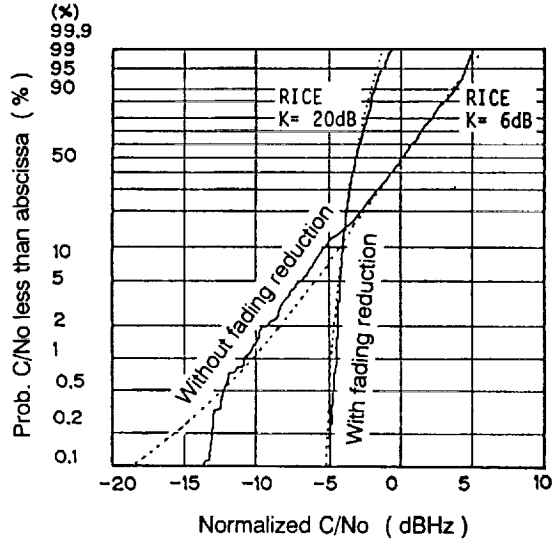

Figure 11 Cumulative distribution of C/No. Dashed lines are the Rician distribution with Rice factors K of 20 dB and 6 dB.

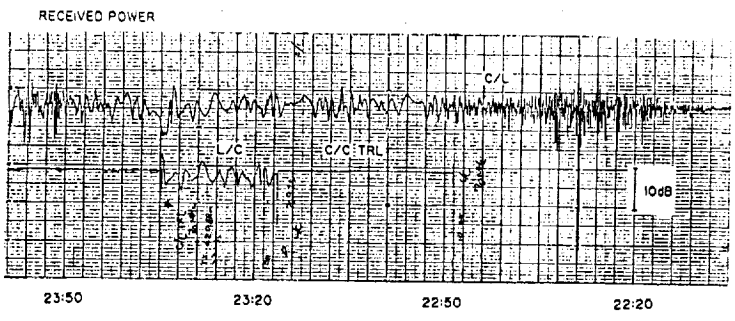

Figure 12 Ionospheric scintillation measured on 30 November 1988.

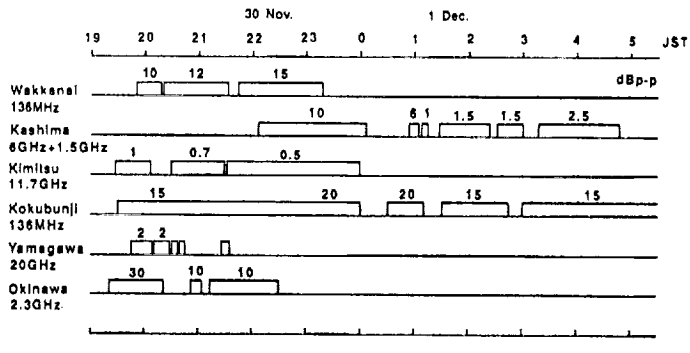

Figure 13 Ionospheric scintillation on 30 Nov., 1988 This figure shows observed places, frequencies and periods when the scintillation occurred.